Published in final edited form as:
Toxicon. 2011 April ; 57(5): 646–656. doi:10.1016/j.toxicon.2011.01.007.

Functional analysis of a recombinant PIII-SVMP, GST-acocostatin; an apoptotic inducer of HUVEC and HeLa, but not SK-Mel-28 cells

Takele Teklemariam[a], **Agustin I. Seoane**[a], **Carla J. Ramos**[a], **Elda E. Sanchez**[b,c], **Sara E. Lucena**[b], **John C. Perez**[b], **Stephanie A. Mandal**[a], and **Julio G. Soto**[a,*]

[a] Biological Sciences Department, San José State University, One Washington Square, San José, CA 95192-0100

[b] National Natural Toxins Research Center, Texas A&M University, Kingsville, TX 78363

[c] Department of Chemistry, Texas A&M University-Kingsville, Kingsville, TX 78363

Abstract

Disintegrins and disintegrin-like peptides interact with integrins and interfere with cell-cell and cell-matrix interactions. A disintegrin-like snake venom gene, *Acocostatin* was cloned from the venom gland mRNA of *Agkistrodon contortrix contortrix*. Acocostatin belongs to the PIII-SVMP subfamily of disintegrin-like peptides. The recombinant acocostatin peptide was produced and purified as GST-fusion. The GST-acocostatin peptide, at 44 μg/mL, inhibited platelet aggregation by 30% in PRP and 18% in whole blood. In addition GST-acocostatin, at 220μg/mL, inhibited SK-Mel-28 cell migration by 48%, but did not inhibit T24 cell migration. The GST-acocostatin peptide ability to induce apoptosis on HUVEC, HeLa, and SK-Mel-28 cells was determined using Annexin-V-FITC and chromatin fragmentation assays after 24 h of treatment. At 5 μM GST-acocostatin peptide, 19.68% +/− 3.09 of treated HUVEC, and 35.86% +/− 2.05 of treated HeLa cells were in early apoptosis. The GST-acocostatin peptide also caused chromatin fragmentation of HUVEC and HeLa cells as determined by fluorescent microscopy and Hoechst staining. The GST-acocostatin peptide failed to induce apoptosis of SK-Mel-28 cells. We characterized the HUVEC, HeLa, and T24 integrin expression by flow cytometry, as the first step in determining GST-acocostatin binding specificity. Our results indicate that HUVEC express αv, αvβ3, αvβ5, α6, β1, and β3 integrin receptors. HeLa cells express α1, α2, α6, αv, αvβ5, and β1 integrin receptors. T24 cells express α1, α3, α6, αv, αvβ3, αvβ5, β1, β3, and β6 integrin receptors.

Keywords

cell adhesion assays; PIII-SVMP; recombinant disintegrin-like; apoptosis

[*]Corresponding author: Julio G. Soto, Biological Sciences Department, San José State University, One Washington Square, San José, CA 95192-0100. jsoto3@email.sjsu.edu, 408-924-4925 (voicemail), 408-924-4840 (FAX).

Conflict of interest statement

The authors declare that there is no conflict of interest.

1. Introduction

Endothelial cells form new blood vessels and are involved in diverse vascular homeostasis processes such as blood clotting, vascular contraction, permeability, and wound healing (Folkman and Shing, 1992). Endothelial cells also engage in pathological conditions such as tumor progression and metastasis because of their role in blood vessel formation that is necessary to deliver oxygen and nutrients to growing tumor cells (Carmeliet and Jain, 2000). Thus, endothelial cells are considered as important targets in the development of anti-cancer therapies (Swenson et al., 2007). Antagonists of integrin receptors have been shown to inhibit angiogenesis and tumor growth by inducing apoptosis of endothelial cells (Brooks et al., 1994; Hsu et al., 2007). Among these antagonists that can be used to prevent tumor cell migration and metastasis are the snake venom toxins called disintegrins (McLane et al., 2004; Swenson et al., 2007).

Disintegrins are small disulfide rich peptides from viper venom that bind to integrins on the surface of normal and malignant cells (Dennis et al., 1990; Gould et al., 1990; McLane et al. 2004). Disintegrin binding motifs include RGD, KGD, MVD, MLD, VGD, and MDG (McLane et al., 2004; Calvete et al., 2005). Disintegrin-integrin binding results in the interference or activation of signal transduction pathways that can be exploited for biomedical research. For example, contortrostatin, a dimeric disintegrin isolated from *Agkistrodon contortrix*, binds to integrins αvβ3 and αvβ5 inhibiting tumor growth and angiogenesis in nude mice (Zhou et al., 2000a; Swenson et al., 2005). The disintegrin DisBa-01 from *Bothrops alternatus* inhibits the adhesion of αvβ3-expressing human microvascular endothelial cell line-1 (HMEC-1) and a murine melanoma cell line (B16F10) to vitronectin, suppressing their proliferation (Ramos et al., 2008).

Non-RGD containing disintegrin-like peptides can also suppress endothelial and tumor cell proliferation by inducing apoptosis. Halysase, a snake venom metalloprotease (SVMP) isolated from the venom of *Gloydius halys*, inhibits the adhesion of endothelial cells to extracellular matrix proteins and induces apoptosis (You et al., 2003a). Other SVMPs such as vascular apoptosis-inducing proteins 1 and 2 (VAP1 and VAP2) (Masuda et al., 1998; Masuda et al., 2000; Maruyama et al., 2005) from the western diamondback rattlesnake (*Crotalus atrox*), and VLAIP (*Vipera lebetina* apoptosis-inducing protein) from *Vipera lebetina* (Trummal et al., 2005) also induce apoptosis of vascular endothelial cells.

SVMPs are proteins that belong to the reprolysin subfamily that contain multiple domains, such as proenzyme domain and a conserved zinc-binding domain (HEXXHXXGXXH) (Fox and Serrano, 2005). Snake venom metalloproteases are classified into three major classes (PI, PII, PIII, and PIV) on the bases of their multi-domain composition, peptide size, and hemorrhagic activities (Fox and Serrano, 2008) . Class PI peptides (20–30kDa) contain only the signal sequence, proenzyme and metalloprotease domains and have relatively weak hemorrhagic activity. Class PII- SVMPs (30–60kDa) contain an additional disintegrin domain in addition to the domains found in class PI. The PIII- SVMPs are high molecular weight (60–100kDa) hemorrhagic peptides that consist of a N-terminal metalloprotease domain, a disintegrin-like domain, and a cysteine-rich domain at the C-terminus.

Research has focused on possible therapeutic and apoptosis inducing applications of SVMPs isolated from crude snake venom (Swenson et al., 2005; Trummal et al., 2005; McLane et al., 2008). Cloning of expressed snake venom genes provides an unlimited source of disintegrin and disintegrin-like SVMPs that may have therapeutic value in the treatment of cancer and other diseases. In the present study, we cloned, expressed, and functionally tested a GST-disintegrin-like snake venom peptide designated as acocostatin, from *Agkistrodon contortrix contortrix*. Recombinant acocostatin is capable of inducing apoptosis of HUVEC

(Human Umbilical Vein Endothelial Cells) and HeLa cells, and preventing cell migration of SK-Mel-28 cells.

2. Materials and methods

2.1. Venom gland sample homogenization, mRNA isolation and Acocostatin cDNA synthesis

A venom gland was obtained from a copperhead snake (Avid # 058–586–284) *Agkistrodon contortrix contortrix*) and frozen at −80°C until mRNA isolation. The venom gland was minced into fine powder under liquid nitrogen using pre-cooled mortar and pestle, and homogenized with a sterile dounce homogenizer. mRNA was isolated using Invitrogen Fast Track 2.0 mRNA isolation kit according to the manufacturer's protocol. RT-PCR reactions were performed to generate double stranded cDNA using Promega Access RT-PCR kit with the following disintegrin specific primer pairs. The forward primer was: 5'CCGGAATTCAAGAGATTGCCTGTCTTCC 3' (an *EcoRI* restriction site is underlined). The reverse primer was: 5'ACGCAAGCTTCTGCCTGTTGCTGCAGAC 3' (a *HindIII* restriction site is underlined). The reverse transcription condition consisted of one cycle at 45°C for 45 min, followed by 94°C for 2 min. The PCR conditions included 40 cycles at 94°C for 30s, 60°C for 1 min and 68°C for 2 min, followed by one cycle of final extension at 68°C for 7 min. The RT-PCR product was purified using the E-gel CloneWell (Invitrogen) electrophoresis apparatus according to the manufacturer's instructions. Purified cDNA bands were sequenced using disintegrin-specific forward and reverse primers (Sequetech Co). Sequencing results were analyzed using Bioedit biological sequence alignment editor version 7.0.9.0. (www.mbio.ncsu.edu/BioEdit/bioedit.html). *Acocostatin* cDNA was translated and the deduced amino acid sequence compared using BLASTp (http://blast.ncbi.nlm.nih.gov*).* The molecular weight of the protein was estimated from the deduced amino acid sequences using the Biology Workbench program (workbench.sdsc.edu).

2.2. Cloning, expression and purification of the GST-acocostatin fusion peptide

Acocostatin cDNA was cloned into the p-GEX (KG) vector. To prepare the GST-acocostatin fusion peptide, samples were transformed into *E. coli* BL21 cells. Cultures were grown to an A_{600} of 0.6–0.8 in 2xYTA broth. After 3 h induction with 1 mM IPTG, cells were centrifuged at 6000 *g* for 15 min at 4 °C. The pellet was resuspended in 20 mL of 1X PBS lysis buffer (140 mM NaCl, 2.7 mM KCl, 10 mM Na_2HPO_4, and 1.8 mM KH_2PO_4, pH 7.3) on ice. Cells were lysed by mild sonication on ice, and centrifuged at 10,000xg for 20 min at 4 °C. The GST-acocostatin fusion peptide was purified in a 5 mL GSTrap column (GE Bioscience) according to the manufacturer's instructions. The concentration of purified peptide was determined with a Bradford assay using bovine serum albumin as a standard. Two micrograms of GST-acocostatin peptide were mixed with 5 μL of 4xNuPAGE LDS sample buffer (Invitrogen) and 2 μL of 10x reducing agent in final volume of 20 μL. The samples were boiled at 70 °C for 10 min, loaded on a NuPAGE 4–12% Bis-Tris gel (Invitrogen), and separated at a constant 200 V for 40 min in NuPAGE 1X MES SDS running buffer (Invitrogen). Three GST-acocostatin peptide purifications were used in this study.

2.3. Inhibition of platelet aggregation using platelet rich plasma (PRP)

Platelet aggregation was estimated by turbidimetry using a dual-channel Chronolog Aggregometer model 560 CA. PRP was prepared by mixing fresh blood sample with trisodium citrate solution (3.2%, w/v) in a volume ratio of 9:1, followed by centrifugation at 190 x *g*, 25°C for 20 min to sediment leukocytes and erythrocytes. The platelet count was adjusted to 3.0×10^8 platelets/mL with platelet-poor plasma. Four hundred and ninety

microliters of citrated PRP were pre-incubated at 37°C with a stir bar in a silicone-treated glass cuvette. Then, 10 μL of GST-acocostatin in PBS buffer or PBS buffer alone were added 4 min before addition of a platelet aggregation inducer. Aggregation was induced by adding 5 μL of ADP (final concentration 10 μM), and the changes in light transmittance were continuously recorded for 6 min. The percentage of inhibition was calculated by comparing light transmittance of GST-acocostatin samples and control.

2.4. Inhibition of platelet aggregation using whole blood

The inhibition of platelet aggregation study was done according to the Sánchez et al. (2010) method using a dual-channel Chrono-Log Whole-Blood Aggregometer [$Ca^{+}2$] model 560 (Havertown, USA). Briefly, different concentrations of GST-acocostatin were added to 10% citrated whole human blood or PRP, and pre-incubated at 37 °C for 2 and 4 min, respectively. Platelet aggregation was initiated by 10 μM ADP. Light transmittance reflecting percentage aggregation was measured using PRP and percentage of impedance was measured using whole blood. The maximal aggregation in the absence of GST-acocostatin was given as 100% aggregation.

2.5. Cell lines and culture conditions

The human melanoma SK-Mel-28 cell line was obtained from ATCC. The SK-Mel-28 cell line was maintained with Eagle's minimum essential medium, supplemented with 10% fetal calf serum in a humidified 5% CO_2 air incubator at 37°C. HUVEC and endothelial cell growth media were purchased from Lonza. HUVEC were cultured in endothelial cell basal medium (EMB-2) supplemented with 0.4% bovine brain extract (BBE), 0.1% human epidermal growth factor (hEGF), 2% fetal bovine serum (FBS), 0.1% hydrocortisone, and 0.1% mL gentomycin, amphoterin B (GA-1000), at 37 °C in 5% CO_2. The growth medium was changed the day after seeding and every other day thereafter. HeLa cells were cultured with DMEM media supplemented with 10% FBS and 1% penicillin-streptomycin-Amphotericin B in a humidified 5% CO_2 air incubator at 37°C. T24 cells were cultured with McCoy's media supplemented with 10% FBS and 1% penicillin-streptomycin-Amphotericin B in a humidified 5% CO_2 air incubator at 37°C.

2.6. Cell migration assay

The migration of tumor cells was measured by cells being scraped from the bottom of the well and measuring the migration. One milliliter ($5.0X10^5$ cells/mL) of T24 and Sk-Mel-28 cells were plated on a 24 well microtiter plate. After 24 h of incubation, the medium was discarded and the confluent monolayer was scratched with a 200 μL sterile tip at the center of the well. The detached cells were washed twice with medium and 1 mL of new medium was added. After the wounding process, the old medium was removed from the wells and replaced by 900 μL of new medium containing 100 μL of GST-acocostatin. Synthetic echistatin at 15 μg/mL (final concentration), a disintegrin that blocked migration of T24 and SK-MEL-28 cells, was used as a positive control. The positive controls prevent tumor cell migration. The negative control consisted of T24 or SK-Mel-28 cells incubated with PBS, which allowed cell migration to occur. The cells were then incubated in a CO_2 chamber and were only removed from the incubator for microscopy images at time 0, 3, 6, 12 and 24 h. Percent of closure was calculated by the following equation: % Closure: [(C–E)/C] × 100, where C is the units of distance of cell edge (mm) at zero time for the control, and E is the distance from the cell edge (mm) at the final incubation time for the disintegrin.

2.7 Cellular adhesion inhibition assay

Inhibition of SK-Mel-28 and T24 cell binding to fibronectin induced by the GST-acocostatin peptide was measured as described previously (Wierzbicka-Patynowski et al., 1999).

Triplicate wells of a 96-well plate were coated with fibronectin at 10μg/mL, in 0.01 M PBS pH 7.4, and incubated overnight at 4°C. The plate was blocked with 0.2 mL of 5% bovine serum albumin (BSA) in PBS and incubated at 37°C, for 1 h. Cells were harvested, counted, and resuspended in medium containing 1% BSA, at 5×10^5 cells/mL. The GST-acocostatin peptide was added to the cell suspension at various concentrations and incubated at 37°C for 1 h. The blocking solution was aspirated, and the cell/protein fraction suspensions (0.2 mL) were added to the wells coated with fibronectin, and incubated at 37°C for 1 h. Synthetic echistatin (SIGMA, Lot. 023K12301), at 3 μM, was used as a positive control. In these wells, 100% of SK-Mel-28 or T24 cells failed to bind to fibronectin. The negative control consisted of SK-Mel-28 or T24 cells incubated with PBS. In these wells, the cells bound to fibronectin. Wells were washed three times with PBS-5% BSA. Two hundred microliters of medium in 1% BSA containing MTT (5:1 vol/vol) were added to the wells containing cells and incubated at 37°C, for 2 h. MTT was aspirated and 100 μL of DMSO were added to lyse the cells. The plate was gently shaken, and the absorbance read at 570 nm using a Beckman Coulter model AD 340 reader. The percent inhibition was calculated by the formula: [(absorbance of negative control – absorbance of cell/venom sample) ÷ absorbance of negative control] × 100.

2.8. Apoptosis Detection

HUVEC, HeLa, and SK-Mel-28 cells were cultured in 24 well plates. Five hundred thousand cells were added to 1 mL of media for each well and grown for 24 h. Three wells in every experiment were dedicated for each different treatment. Experiments were performed in triplicates. After initial incubation, wells were treated with either, 5μM GST or GST-acocostatin peptide and incubated for 24 h. An untreated control was also performed. Cells were then detached from the plate surface using 0.05% trypsin EDTA. Trypsin was neutralized with culture media. Cells were centrifuged, washed twice with cold PBS, and resuspended in 250 μL of 1X binding buffer. Then, 100 μL were removed and exposed to 5 mL each of Annexin-V-FITC and Propidium Iodide, PI (BD Biosciences). The reaction was incubated at room temperature, in the dark for 15 min. Four hundred microliters of 1X binding buffer were added and 10,000 events per sample were analyzed using a Becton Dickinson FACScan flow cytometer and FACSCalibur software. Statistical analysis of the percent apoptotic cell population, using ANOVA, was performed using Systat.

2.9. Chromatin Fragmentation

HUVEC and HeLa cells were grown on chambered slides. One and a half million cells were grown in 2 mL of media and grown for 24 h. After initial incubation, cells were treated with either, 5μM GST or GST-acocostatin peptide for 24 h. An untreated control was also performed. The media was aspirated and the cells washed twice with 1X PBS. Cells were fixed on the slide with 3% formaldehyde for 1 h, followed by two washes with 1X PBS. Ten micrograms/mL of Hoechst stain was added to cells and incubated in the dark for 15 min. Excess Hoechst stain was removed by two 1X PBS washes. Slides were mounted with 30% glycerol and viewed at 100X, oil immersion, with a Zeiss AXIO fluorescent microscope.

2.10. Characterization of integrins expression on HUVEC, HeLa, and T24 cells with flow cytometry

The following antibodies were used to determine integrin expression on HUVEC, HeLa, and T24 cells. Antibodies against αvβ3 (αvβ3 sc-7312-FITC), α1 (α1 sc-81733-FITC), α2 (α2 sc-53352-FITC), α3 (α3 sc-13545-FITC), α6 (α6 sc-19622-FITC), αv (αv-53360-FITC), β1 (β1 sc-9970-FITC), β3 (β3 sc-51738-FITC), CD9 (CD9 sc-13118-FITC), and respective isotypes were purchased from Santa Cruz Biotechnology. Antibodies against αvβ5 (MAB1961F) were purchased from Millipore. Cells were cultured to 90–95% confluency in a 75 cm^2 tissue culture flask and detached from the flask surface using 0.05% trypsin

EDTA. Trypsin was neutralized with complete culture media. Cells were resuspended in 1X PBS to a final concentration of 10^6 cells/mL, and blocked with 1 μL/mL normal rabbit serum, for 25 min at room temperature. After blocking, cells were washed with 1mL 1X PBS, centrifuged, and resuspended in FCM Wash Buffer (Santa Cruz Biotechnology) to 10^6 cells/mL. One hundred microliters of cells were distributed in three, 12 × 75 mm round bottom glass test tubes and fixed in 1% formaldehyde for 1 h. After fixation, cells were washed three times in 1X PBS. The first tube received 5–20 μL of a cocktail containing fluorochrome-conjugated monoclonal antibody. The second tube received the same volume of matched isotype control antibody. The third tube of cells received an equivalent volume of 1X PBS. This served as an autofluorescence control to establish appropriate flow cytometer settings. Cells were incubated with conjugated antibodies or control for 1 h, at room temperature, in the dark. Then three washes with 1X PBS were performed to remove unbound antibodies. Four hundred microliters of 1X binding buffer were added and the samples analyzed using a Becton Dickinson FACScan flow cytometer and FACSCalibur software.

3. Results

3.1. Disintegrin cDNA RT-PCR and sequence analysis

Two cDNAs (212 bp and 417 bp) were obtained from the RT-PCR primers. For this study, we cloned and expressed the 417 bp cDNA (designated as *Acocostatin*, GenBank accession# HQ206717), a PIII-SVMP. The PIII-SVMP identified in this study is coded by a truncated cDNA. Isoleucine is the first codon of the *Acocostatin* cDNA. This cDNA lacks a stop codon, and produces a 139 amino acid long peptide (Fig. 1). The translated peptide contains a disintegrin-like region containing an Asp-Glu-Cys-Asp (DECD) motif, a cysteine-rich region containing 20 cysteine residues, a variable region (10 amino acids) and a truncated hypervariable region (two amino acids) at the C-terminus.

3.2. Production and purification of the GST-acocostatin peptide

Recombinant GST-acocostatin peptide was expressed in BL21 *E. coli* cells and purified. The purified recombinant GST-acocostatin fusion peptide produced a single band at 42 kDa when analyzed with SDS-PAGE under reducing conditions (Fig 2). GST alone separated at 26 kDa, as determined by SDS-PAGE. Thus, the estimated molecular mass of acocostatin using SDS-PAGE was 16 kDa.

3.3. Inhibition of platelet aggregation and cell migration activities of GST-acocostatin

The GST-acocostatin peptide inhibited platelet aggregation by 33% in PRP and 18% in whole blood (Table 1). In addition GST-acocostatin inhibited SK-Mel-28 cell migration by 48% (Table 2).

3.4. The GST-acocostatin peptide induced apoptosis of HUVEC and HeLa cells

The GST-acocostatin peptide's ability to induce apoptosis on HUVEC, HeLa, and SK-Mel-28 cells was determined using Annexin V-FITC and chromatin fragmentation assays. Since acocostatin was produced as a fusion with GST, it was essential to verify if GST contributed to apoptosis induction. To exclude that possibility, we tested GST recombinant protein alone under similar conditions. The results indicated that GST alone produced less than 5% of early apoptotic cells, which was comparable to the rate observed in untreated cells. Therefore, GST did not contribute in the induction of apoptosis of HUVEC or HeLa cells in the GST-acocostatin peptide.

Fig. 3 shows quantification results of early apoptosis from triplicate experiments. At 5 μM GST-acocostatin peptide, 19.68% +/− 3.09 of treated HUVEC, and 35.86% +/− 2.05 of

treated HeLa cells were in early apoptosis. The GST-acocostatin peptide failed to induce apoptosis of SK-Mel-28 cells.

The GST-acocostatin peptide was also able to induce chromatin fragmentation as determined by fluorescent microscopy and Hoechst staining (Fig. 4A–C). Nuclear fragmentation was not detected in untreated cells (Fig. 4C), or cells treated with GST-only protein (data not shown).

3.5. Characterization of integrin expression on HUVEC, HeLa, and T24 cells

Flow cytometry was used to characterize integrin expression on HUVEC, HeLa, and T24 cells, as the first step in determining which integrins bind to GST-acocostatin. Our results showed that HUVEC express α3, α6, αv, αvβ3, αvβ5, β1, and β3 integrin receptors (Fig. 5). HeLa cells express α1, α2, α6, αv, αvβ5, and β1 integrin receptors. T24 cells express α1 (at very low levels), α3, α6, αv, αvβ3, αvβ5 (at very low levels), β1, and β3, integrin receptors.

4. Discussion

Snake venom contains a variety of active peptides including the high molecular weight PIII-SVMPs. PIII-SVMPs contain metalloprotease, disintegrin-like, and cysteine-rich domains (Calvete et al., 2005). These high molecular weight SVMPs are involved in proteolytic degradation of extracellular proteins, inhibition of collagen-induced platelet aggregation, and induction of endothelial cell apoptosis (You et al., 2003a; You et al., 2003b; You et al., 2006).

4.1. Acocostatin is a truncated PIII-SVMP

RT-PCR amplification of *A. contortrix contortrix* snake venom mRNA with disintegrin specific primers produced two different cDNA products (a 212 bp and a 417 bp bands). This is due to high homology between the different disintegrin genes that can be amplified with the same primers. The 212 bp cDNA showed 93% identity with *Acostatin* (*Agkistrodon contortrix contortrix*, accession# AB078904) and 92% identity with *Piscivostatin* (*Agkistrodon piscivorus piscivorus* accession # AB078906). The 417 bp cDNA revealed 95% nucleotide identity with *Crotastatin* (*Crotalus durissus terrificus*, accession# DQ224420) and 94% identity with *Vascular apoptosis-1* (*VAP1*) (*Crotalus atrox*, AB042840).

In this study, we cloned and expressed the 417 bp cDNA (designated as *Acocostatin*). Analysis of the predicted amino acid sequence revealed that acocostatin is composed of a truncated PIII-SVMP containing the disintegrin-like domain and part of the cysteine-rich domain. The disintegrin-like domain of acocostatin contains an ECD motif, which is similar to other previously reported PIII-SVMPs such as VAP1 from *Crotalus atrox* (Masuda et al., 2000) and halysase from *Gloydius halys* (You et al., 2003a). Figure 6 shows an amino acid sequence comparison of acocostatin with other closely related PIII-SVMPs. CLUSTAL W multiple sequence alignment revealed that acocostatin shares 93% amino acid identity with VAP1 (accession # BAB18307), crotastatin-1 (accession # ACI02286), lachestatin-2 (accession # ACI02291), batroxstatin-2 (accession # ACI02288), lachestatin-1 (accession # ACI02290), and 92% identity with metalloproteinase isoform-7 (accession # ABG26984). Cysteine residues are conserved in all sequences.

4.2. GST-disintegrin peptides have biological activity

GST-disintegrin or-disintegrin-like fusion peptides have biological activity. Functional studies performed with GST-elegantin (Rahman et al., 1998), GST-rhodostomin (Chang et al., 1993), GST-Adam 9 disintegrin peptide (Mahimkar et al., 2005), and GST-Moj peptides

(Seoane et al., 2010) demonstrated that disintegrin peptides fused to GST are functional. Furthermore, the activity of recombinant rhodostomin in binding competition assays suggested that the GST-rhodostomin peptide was properly folded (Chang et al., 1993).

Moreover, GST-fusions were used to study the role of the disintegrin-like and cysteine-rich regions of the PIII-SVMP, HF3, on leukocyte rolling (Menezes et al., 2008). The GST-DC (the disintegrin and cysteine-rich region together) and GST-C (cysteine-rich region only) peptides activated leukocyte rolling and leukocyte adhesion to endothelial tissue. However, the GST and GST-D (disintegrin region only) peptides failed to activate leukocyte rolling or leukocyte adhesion, demonstrating that the results obtained from the GST-fusion peptides were specific to the HF3 sequence examined and not to the GST fusion partner.

4.3. The GST-acocostatin peptide induced apoptosis of HUVEC, HeLa, but not Sk-Mel-28 cells

Apoptosis induction activity by the GST-acocostatin peptide was cell-specific. Although apoptosis was induced in both HUVEC and HeLa cells, the GST-acocostatin peptide was more effective in inducing a higher percentage of HeLa cells to undergo apoptosis (Fig. 3). Furthermore, the human melanoma cell line, SK-Mel-28, failed to undergo apoptosis after 24 h treatment with 5μM GST-acocostatin.

Apoptosis induction activity of GST-acocostatin on HUVEC was lower than previously reported apoptotic activity from other PIII-SVMPs. For instance after 24 h of incubation, recombinant (r) halysase (10 nM) and VLAIP (10 μg/ml) induced apoptosis of 70% and 35% of HUVEC treated, respectively (You et al., 2003a; Trummal et al., 2005). The difference in activity between GST-acocostatin, r-halysase, and VLAIP can be attributed to the following differences. First, the method of apoptosis quantification was different in all three studies. You et al., (2003a) determined the percentage of cells undergoing apoptosis by counting apoptotic cells with a fluorescent microscope. This method of quantification fails to discriminate between early and late stages of apoptosis and hence may contribute to a higher percentage of apoptotic cells reported. In our study, we double stained our treated cells with PI and Annexin V in order to distinguish between early apoptosis and necrosis/late apoptosis induction. Trummal et al. (2005) only used Annexin V single staining. Therefore, it is possible that the higher percentage of apoptotic cells they obtained was a mixture of early to late stages of apoptosis and probably, necrotic cells. Second, GST-acocostatin sequence is truncated and lacks the metalloprotease domain and the C-terminus. It has been shown that the metalloprotease domain contributes to the apoptotic activity of r-halisase (You et al., 2003a).

Morphological changes such as chromatin fragmentation, cell shrinkage, and the formation of cellular blebs associated with apoptosis induction were observed in HUVEC and HeLa cells treated with the GST-acocostatin peptide. Similar results were obtained with HUVEC treated with VAP1 (Masuda et al., 2000), r-halysase (You et al., 2003a).

4.4. Possible binding targets of GST-acocostatin

Integrins are a family of cell surface glycoproteins that occur in different alpha and beta combinations. They regulate different cellular functions such as adhesion, proliferation, differentiation, and migration (Huveneers et al., 2007). The different a and β subunits combine to form distinct integrins that are expressed in a wide variety of tissues that have different affinities for different ECM proteins (Hynes, 1992). Integrins recognize the RGD sequences in the ECM proteins and involve in the bidirectional signal transduction that can alter different cellular events (Swenson et al., 2007). The involvement of integrins in various pathological conditions is also well established. For example, integrins αvβ3 and αvβ5 have

been implicated to play a role in apoptosis, angiogenesis, tumor growth, and metastasis (Brooks et al., 1994; Eliceiri and Cheresh, 1999; Hood and Cheresh, 2002). The role of integrins in cancer progression has led investigators to focus on finding and characterizing molecules that block integrin mediated signaling and inhibit tumor progression.

In addition to affecting platelet aggregation, disintegrins inhibit adhesion, migration and proliferation of cells by binding to integrins that are expressed on platelets, vascular endothelial cells, and tumor cells (Brooks et al., 1995; Zhou et al., 2000b; Marcinkiewicz et al., 2003; McLane et al., 2004). These interactions occur between the disintegrins RGD motif and integrins that are expressed on the surface of both normal and cancer cells (You et al., 2003a; Swenson et al., 2005) . Disintegrins act as competitive inhibitors of cell surface ligands on cancer cells and alter cell-cell and cell-matrix interactions (Swenson et al., 2004; Yang et al., 2005; McLane et al., 2008).

Araki et al. (2002) utilized antibody-blocking experiments to infer VAP1 binding specificity. They reported that VAP1 induce apoptosis of HUVEC through α3, α6, β1 integrins and CD9, a transmembrane protein usually associated with integrin receptors. Although acocostatin and VAP1 share 93% amino acid identity, their binding specificity may not be similar. Our data suggest that GST-acocostatin does not utilize the α2, α6, or β1 receptors to induce apoptosis of HUVEC and HeLa cells since these receptors are expressed on SK-Mel-28 (Fig. 5, this study; Seoane et al., 2010), a cell line that failed to undergo apoptosis after GST-acocostatin treatment. In addition, α3 or αvβ3 are not utilized by GST-acocostatin's induction of apoptosis on HeLa cells. The α3 receptor is not expressed on HeLa, and the αvβ3 receptor is absent on this cell line and present on Sk-Mel-28 (Seoane et al., 2010). Finally, we were unable to detect CD9 on the surface of HUVEC and suggest that CD9 probably is not involved in the activation of HUVEC apoptosis (Fig. 7B).

A possible integrin target for GST-acocostatin binding and apoptosis activation of HUVEC and HeLa cells may be αvβ5, a receptor found on both cell lines but not on Sk-Mel-28. Integrin αvβ5 binds to vitronectin (Moschos et al., 2007), and its expression has been correlated with cancer aggressiveness of some invasive tumors (Radis-Baptista, 2005). Although the αvβ5 receptor recognizes the RGD motif (Barczyk et al., 2010), there are several peptides that lack RGD and bind to this receptor. For instance, syndecan-1 (Sdc1) and the CXC-chemokine CXCL4 are non-RGD containing peptides that bind to αvβ5 and regulate angiogenesis (Beauvais et al., 2009; Aidoudi et al., 2008). Beauvais et al. (2009) suggests that Sdc-1 binds to αvβ5 laterally inducing clustering of αvβ5 receptors. However, CXCL4 may bind directly to the binding site of αvβ5, as antibody blocking experiments against αvβ5 demonstrated that HUVEC binding to immobilized CXCL4 is blocked (Aidoudi et al., 2008). Other proteins, such as βig-h3 and Thy-1 (thymus cell antigen 1), bind to αvβ5 using different motifs even when they contain an RGD. Several of the periostin family of proteins, such as βig-h3 and periostin, bind to αvβ5 receptors via YH or Asp-Ile motifs (Litvin et al., 2005; Guohong et al., 2010). Thy-1 binds to αvβ5 on lung fibroblasts via an RLD sequence (Zhou et al., 2010).

GST-acocostatin was unable to induce apoptosis of SK-Mel-28 cells, but inhibited the migration of this cell line. The cell migration inhibition was cell specific, as GST-acocostatin failed to inhibit T24 cell migration. Predicting the receptor that may be targeted by GST-acocostatin to inhibit cell migration of SK-Mel-28 cells is difficult at present. For contortrostatin, a dimeric disintegrin, its interaction with αvβ3 and αvβ5 integrins may lead to inhibition of breast cancer cell migration (Swenson et al., 2004; Swenson et al., 2007). SK-Mel-28 and T24 cell lines express the αvβ3 integrin receptor, but the αvβ5 is expressed on T24 but not on SK-Mel-28 (Seoane et al., 2010; and Fig.5, this study).

Crystallography studies of two PIII-SVMPs (VAP1 and catrocollastatin/VAP2B) indicate that their disintegrin-like loop is not accessible for integrin binding (Takeda et al., 2006; Igarashi et al., 2007). Furthermore, they suggested that a hypervariable region, 12 amino acids carboxyl of the variable region (at the cysteine rich domain), is a potential integrin binding site. Functional studies demonstrated that the cysteine-rich region at the C-terminus of PIII-SVMPs is a site for binding to collagen type I, and platelet aggregation inhibition (Jia et al., 2000; Pinto et al., 2007; Serrano et al., 2007). Pinto et al. (2006) found that the sequence capable of blocking platelet aggregation is located within the hypervariable region of jararhagin, a PIII-SVMP. This region can potentially bind to α2β1 integrin receptors preventing platelet aggregation (Kamiguti et al., 2003). Other PIII-SVMPs bind to α2β1 integrin, a known collagen receptor on platelets (You et al., 2003a; Selistre-de-Araujo et al., 2005). However, not all PIII-SVMPs block collagen binding. For instance, VAP1 does not bind to collagen and when the α2 integrin receptor on HUVEC was blocked with antibodies, VAP1 was able to induce apoptosis (Araki et al., 2002).

4.5. Conclusions

The truncated version of acocostatin in our study lacks the metalloprotease domain and 13 amino acids at the N-terminus of the disintegrin-like domain. It has a variable region in the cysteine-rich domain and the first two amino acids of the hypervariable region (Fig 6). Data from our study and others suggest that not all of the possible binding sites of PIII-SVMPs are found at the hypervariable region. For instance, halydin, a disintegrin-like peptide lacking the variable and hypervariable regions, blocked platelet aggregation when whole blood was used, by interrupting collagen binding to the α1β1 receptor on platelets (You et al., 2003b). Our peptide blocked platelet aggregation of whole blood and PRP suggesting that acocostatin's hypervariable region may not be used in the inhibition of platelet aggregation. Takeda et al. (2006) suggested that the PIII-SVMPs variable region, consisting of 10 residues, on the cysteine rich domain might be a site of protein binding. It is possible that the integrin binding site of GST-acocostatin may be in its variable region as our study shows that GST-acocostatin is able to induce apoptosis and prevent cell migration in the absence of most of the hypervariable region.

Acknowledgments

We thank Cleber Ouverney and Lucy Arispe for technical assistance. Funding for this project was provided by NIH/SCORE # 2SO6 GM008192, NIH/RISE Grant# 5R25GM071381, NIH-NIGMS Minority Access to Research Careers (MARC) # 5T34GM 08253, NIH/SCORE # 2SO6 GM008192, NCRR/Viper # 2P40RR018300, NIH/RIMI #5 5P20MD000216, and NIH/SCORE #5 S06 GM0081079.

LITERATURE CITED

Aidoudi A, Bujakowski K, Kieffer N, Bikfalvi A. The CXC-chemokine CXCL4 interacts with integrins implicated with angiogenesis. PLOS one. 2008; 3:1–14.

Araki S, Masuda S, Maeda H, Ying MJ, Hayashi H. Involvement of specific integrins in apoptosis induced by vascular apoptosis-inducing protein 1. Toxicon. 2002; 40:535–542. [PubMed: 11821125]

Barczyk M, Carracedo S, Gullberg D. Integrins. Cell Tissue Res. 2010; 339:269–280. [PubMed: 19693543]

Beauvais DM, Ell BJ, McWhorter AR, Rapraeger AC. Syndecan-1 regulates αvβ3 and αvβ5 integrin activation during angiogenesis and is blocked by synstatin, a novel peptide inhibitor. J Exp Med. 2009; 206:691–705. [PubMed: 19255147]

Brooks PC, Montgomery AM, Rosenfeld M, Reisfeld RA, Hu T, Klier G, Cheresh DA. Integrin alpha v beta 3 antagonists promote tumor regression by inducing apoptosis of angiogenic blood vessels. Cell. 1994; 79:1157–1164. [PubMed: 7528107]

Brooks PC, Stromblad S, Klemke R, Visscher D, Sarkar FH, Cheresh DA. Anti-integrin alpha v beta 3 blocks human breast cancer growth and angiogenesis in human skin. J Clin Invest. 1995; 96:1815–1822. [PubMed: 7560073]

Calvete JJ. Structure-function correlations of snake venom disintegrins. Curr Pharm Des. 2005; 11:829–835. [PubMed: 15777237]

Calvete JJ, Marcinkiewicz C, Monleon D, Esteve V, Celda B, Juarez P, Sanz L. Snake venom disintegrins: evolution of structure and function. Toxicon. 2005; 45:1063–1074. [PubMed: 15922775]

Carmeliet P, Jain RK. Angiogenesis in cancer and other diseases. Nature. 2000; 407:249–257. [PubMed: 11001068]

Chang HH, Hu ST, Huang TF, Chen SH, Lee YH, Lo SJ. Rhodostomin, an RGD-containing peptide expressed from a synthetic gene in Escherichia coli, facilitates the attachment of human hepatoma cells. Biochem Biophys Res Commun. 1993; 190:242–249. [PubMed: 7916592]

Dennis MS, Henzel WJ, Pitti RM, Lipari MT, Napier MA, Deisher TA, Bunting S, Lazarus RA. Platelet glycoprotein IIb-IIIa protein antagonists from snake venoms: evidence for a family of platelet-aggregation inhibitors. Proc Natl Acad Sci U S A. 1990; 87:2471–2475. [PubMed: 2320569]

Eliceiri BP, Cheresh DA. The role of alphav integrins during angiogenesis: insights into potential mechanisms of action and clinical development. J Clin Invest. 1999; 103:1227–1230. [PubMed: 10225964]

Folkman J, Shing Y. Angiogenesis. J Biol Chem. 1992; 267:10931–10934. [PubMed: 1375931]

Fox JW, Serrano SM. Structural considerations of the snake venom metalloproteinases, key members of the M12 reprolysin family of metalloproteinases. Toxicon. 2005; 45:969–985. [PubMed: 15922769]

Fox JW, Serrano SM. Insights and speculations into snake venom metalloproteinase (SVMP) synthesis, folding and disulfide bond formation and their contribution to venom complexity. FEBS J. 2008; 275:3016–3030. [PubMed: 18479462]

Gould RJ, Polokoff MA, Friedman PA, Huang TF, Holt JC, Cook JJ, Niewiarowski S. Disintegrins: a family of integrin inhibitory proteins from viper venoms. Proc Soc Exp Biol Med. 1990; 195:168–171. [PubMed: 2236100]

Guohong L, Jin R, Norris RA, Zhang L, Yu S, Wu F, Markwald RR, Nanda A, Conway SJ, Smyth SB, Granger DN. Periostin mediates smooth muscle migration through the integrins αvβ3 and αvβ5 and focal adhesion kinase (FAK) pathway. Atheriosclerosis. 2010; 208:358–365.

Hood JD, Cheresh DA. Role of integrins in cell invasion and migration. Nat Rev Cancer. 2002; 2:91–100. [PubMed: 12635172]

Hsu AR, Veeravagu A, Cai W, Hou LC, Tse V, Chen X. Integrin alpha v beta 3 antagonists for anti-angiogenic cancer treatment. Recent Pat Anticancer Drug Discov. 2007; 2:143–158. [PubMed: 18221059]

Huveneers S, Truong H, Danen HJ. Integrins: signaling, disease, and therapy. Int J Radiat Biol. 2007; 83:743–751. [PubMed: 17852562]

Hynes RO. Integrins: versatility, modulation, and signaling in cell adhesion. Cell. 1992; 69:11–25. [PubMed: 1555235]

Igarashi T, Araki S, Mori H, Takeda S. Crystal structures of catrocollastatin/VAP2B reveal a dynamic, modular architecture of ADAM/adamalysin/reprolysin family proteins. FEBS Lett. 2007; 581:2416–2422. [PubMed: 17485084]

Jia LG, Wang XM, Shannon JD, Bjarnason JB, Fox JW. Inhibition of platelet aggregation by the recombinant cysteine-rich domain of the hemorrhagic snake venom methalloproteinase, atrolysin-A. Arch Biochem Biophys. 2000; 373:281–286. [PubMed: 10620350]

Kamigutti AS, Gallagher P, Marcinkiewicz C, Theaskston RD, Zuzel M, Fox JW. Identification of sites in the cysteine-rich domain of the class PIII snake venom methalloproteinases responsible for inhibition of platelet function. FEBS Lett. 2003; 549:129–134. [PubMed: 12914938]

Litvin J, Zhu S, Norris R, Markwald R. Periostin family of proteins: therapeutic targets for heart disease. Anat Rec A Mol Cell Evol Biol. 2005; 287A:1205–1212.

Mahimkar RM, Visaya O, Pollock AS, Lovett DH. The disintegrin domain of ADAM9: a ligand for multiple beta1 renal integrins. Biochem J. 2005; 385:461–468. [PubMed: 15361064]

Marcinkiewicz C, Weinreb PH, Calvete JJ, Kisiel DG, Mousa SA, Tuszynski GP, Lobb RR. Obtustatin: a potent selective inhibitor of alpha1beta1 integrin in vitro and angiogenesis in vivo. Cancer Res. 2003; 63:2020–2023. [PubMed: 12727812]

Maruyama J, Hayashi H, Miao J, Sawada H, Araki S. Severe cell fragmentation in the endothelial cell apoptosis induced by snake apoptosis toxin VAP1 is an apoptotic characteristic controlled by caspases. Toxicon. 2005; 46:1–6. [PubMed: 15922392]

Masuda S, Hayashi H, Araki S. Two vascular apoptosis-inducing proteins from snake venom are members of the metalloprotease/disintegrin family. Eur J Biochem. 1998; 253:36–41. [PubMed: 9578458]

Masuda S, Ohta T, Kaji K, Fox JW, Hayashi H, Araki S. cDNA cloning and characterization of vascular apoptosis-inducing protein 1. Biochem Biophys Res Commun. 2000; 278:197–204. [PubMed: 11071872]

McLane MA, Sanchez EE, Wong A, Paquette-Straub C, Perez JC. Disintegrins. Curr Drug Targets Cardiovasc Haematol Disord. 2004; 4:327–355. [PubMed: 15578957]

McLane MA, Joerger T, Mahmoud A. Disintegrins in health and disease. Front Biosci. 2008; 13:6617–6637. [PubMed: 18508683]

Menezes MC, Paes ADL, Melo RL, Silva CA, Della Casa M, Bruni FM, Lima C, Lopes-Ferreira M, Camargo ACM, Fox JW, Serrano SMT. Activation of leukocyte rolling by the cysteine-rich domain and the hypervariable region HF3, a snake venom hemorrhagic metalloproteinase. FEBS Lett. 2008; 582:3915–3921. [PubMed: 18977230]

Moschos SJ, Drogowski LM, Reppert SI, Kirkwood JM. Integrins and cancer. Oncology. 2007; 21:13–20. [PubMed: 17927026]

Pinto AFM, Terra RMS, Guimaraes JA, Fox JW. Mapping von Willerand factor A domain binding sites on a snake venom metalloproteinase cysteine-rich domain. Arch Biochem Biophys. 2007; 457:41–46. [PubMed: 17118332]

Radis-Baptista G. Integrins, cancer and snake toxins (mini-review). J Venom Anim Toxins incl Trop Dis. 2005; 11:217–241.

Rahman S, Aitken A, Flynn G, Formstone C, Savidge GF. Modulation of RGD sequence motifs regulates disintegrin recognition of alphaIIb beta3 and alpha5 beta1 integrin complexes. Replacement of elegantin alanine-50 with proline, N-terminal to the RGD sequence, diminishes recognition of the alpha5 beta1 complex with restoration induced by Mn2+ cation. Biochem J. 1998; 335:247–257. [PubMed: 9761721]

Ramos OH, Kauskot A, Cominetti MR, Bechyne I, Salla Pontes CL, Chareyre F, Manent J, Vassy R, Giovannini M, Legrand C, Selistre-de-Araujo HS, Crepin M, Bonnefoy A. A novel alpha(v)beta (3)-blocking disintegrin containing the RGD motive, DisBa-01, inhibits bFGF-induced angiogenesis and melanoma metastasis. Clin Exp Metastasis. 2008; 25:53–64. [PubMed: 17952617]

Sanchez EE, Lucena SE, Reyes S, Soto JG, Cantu E, Lopez-Johnston JC, Guerrero B, Salazar AM, Rodriguez-Acosta A, Galan JA, Tao WA, Perez JC. Cloning, expression, and hemostatic activities of a disintegrin, r-mojastin 1, from the mohave rattlesnake (Crotalus scutulatus scutulatus). Thromb Res. 2010; 126:211–219. [PubMed: 20667584]

Selistre-de-Araujo HS, Cominetti MR, Terrugi CHB, Mariano-Olivera A, De Freitas MS, Crepin M, Figueiredo CC, Morandi V. Alternagin-C, a disintegrin-like protein from the venom of Bothrops alternatus, modulates α2β1 integrin-mediated cell adhesion, migration, and proliferation. Brazilian J Med Biol Research. 2005; 38:1505–1511.

Seoane AI, Tran VL, Sanchez EE, White SA, Choi JL, Gaytán B, Chavez N, Reyes SR, Ramos CJ, Tran LH, Lucena SE, Sugarrek M, Perez JC, Mandal SA, Ghorab S, Rodriguez-Acosta A, Fung BK, Soto JG. The mojastin mutant Moj-DM induces apoptosis of the human melanoma Sk-Mel-28, but not the mutant Moj-NN nor the non-mutated recombinant Moj-WN. Toxicon. 2010; 56:391–401. [PubMed: 20398687]

Serrano AMT, Wang D, Shannon JD, Pinto AFM, Polanowska-Grabowska RK, Fox JW. Interaction of the cysteine-rich domain of snake venom methalloproteinase with the A1 domain of von

Willebrand factor promotes site-specific proteolysis of von Willebrand factor and inhibition of von Willebrand factor-mediated platelet aggregation. FEBS J. 2007; 274:3611–3621. [PubMed: 17578514]

Swenson S, Costa F, Minea R, Sherwin RP, Ernst W, Fujii G, Yang D, Markland FS Jr. Intravenous liposomal delivery of the snake venom disintegrin contortrostatin limits breast cancer progression. Mol Cancer Ther. 2004; 3:499–511. [PubMed: 15078994]

Swenson S, Costa F, Ernst W, Fujii G, Markland FS. Contortrostatin, a snake venom disintegrin with anti-angiogenic and anti-tumor activity. Pathophysiol Haemost Thromb. 2005; 34:169–176. [PubMed: 16707922]

Swenson S, Ramu S, Markland FS. Anti-angiogenesis and RGD-containing snake venom disintegrins. Curr Pharm Des. 2007; 13:2860–2871. [PubMed: 17979731]

Takeda S, Igarashi T, Mori H, Araki S. Crystal structures of VAP1 reveal ADAMs' MDC domain architecture and its unique C-shaped scaffold. The EMBO J. 2006; 25:2388–2396.

Trummal K, Tonismagi K, Siigur E, Aaspollu A, Lopp A, Sillat T, Saat R, Kasak L, Tammiste I, Kogerman P, Kalkkinen N, Siigur J. A novel metalloprotease from Vipera lebetina venom induces human endothelial cell apoptosis. Toxicon. 2005; 46:46–61. [PubMed: 15922394]

Wierzbicka-Patynowski I, Niewiarowski S, Marcinkiewicz C, Calvete JJ, Marcinkiewicz MM, McLane MA. Structural requirements of echistatin for the recognition of alpha(v)beta(3) and alpha(5)beta(1) integrins. J Biol Chem. 1999; 274:37809–37814. [PubMed: 10608843]

Yang RS, Tang CH, Chuang WJ, Huang TH, Peng HC, Huang TF, Fu WM. Inhibition of tumor formation by snake venom disintegrin. Toxicon. 2005; 45:661–669. [PubMed: 15777962]

You WK, Jang YJ, Chung KH, Kim DS. A novel disintegrin-like domain of a high molecular weight metalloprotease inhibits platelet aggregation. Biochem Biophys Res Commun. 2003a; 309:637–642. [PubMed: 12963038]

You WK, Seo HJ, Chung KH, Kim DS. A novel metalloprotease from Gloydius halys venom induces endothelial cell apoptosis through its protease and disintegrin-like domains. J Biochem. 2003b; 134:739–749. [PubMed: 14688240]

You WK, Jang YJ, Chung KH, Jeon OH, Kim DS. Functional roles of the two distinct domains of halysase, a snake venom metalloprotease, to inhibit human platelet aggregation. Biochem Biophys Res Commun. 2006; 339:964–970. [PubMed: 16329990]

Zhou Q, Nakada MT, Brooks PC, Swenson SD, Ritter MR, Argounova S, Arnold C, Markland FS. Contortrostatin, a homodimeric disintegrin, binds to integrin alphavbeta5. Biochem Biophys Res Commun. 2000a; 267:350–355. [PubMed: 10623623]

Zhou Q, Sherwin RP, Parrish C, Richters V, Groshen SG, Tsao-Wei D, Markland FS. Contortrostatin, a dimeric disintegrin from Agkistrodon contortrix contortrix, inhibits breast cancer progression. Breast Cancer Res Treat. 2000b; 61:249–260. [PubMed: 10966001]

Zhou Y, Hagood JS, Lu B, Merryman WD, Murphy-Ulrich JE. Thy-1- Integrin αvβ5 interactions inhibit lung fibroblast contraction-induced latent transforming growth factor-β1 activation and myofibroblast differentiation. J Biol Chem. 2010; 285:22382–22393. [PubMed: 20463011]

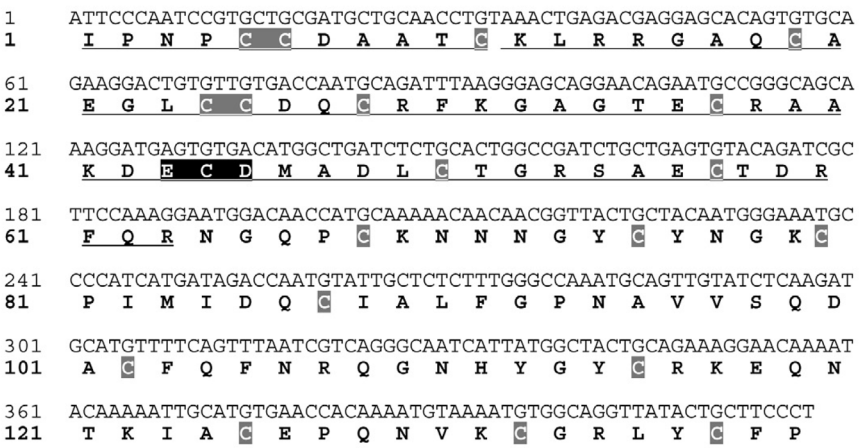

Fig.1.

cDNA sequence and predicted amino acid sequence of acocostatin. The cDNA sequences are located on the upper line and the predicted amino acid sequences denoted by one letter symbol are situated on the lower line. The cysteine residues are shaded in gray boxes and the ECD motif is shaded in black.

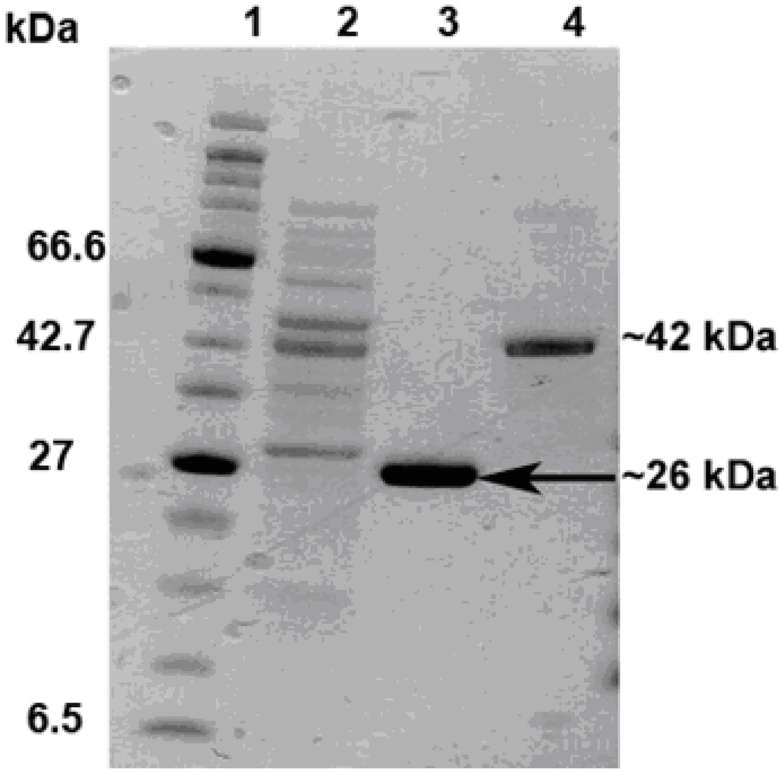

Fig. 2.

SDS-PAGE of expressed protein resolved in a 4–12 % NuPAGE Bis-Tris gel under reducing condition. Molecular weight marker (Lane 1). Induced bacterial whole lysate expressing GST-acocostatin fusion protein (Lane 2). Affinity purified GST protein (Lane 3). Affinity purified GST-acocostatin fusion protein (Lane 4).

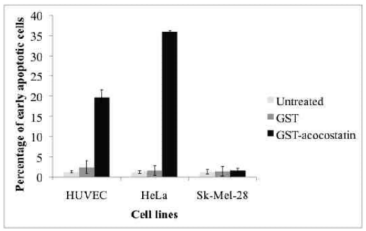

Fig. 3.

GST-acocostatin induced apoptosis of HUVEC, HeLa, but nor Sk-Mel–28 cells. Cells were cultured for 24 h with either medium alone, 5 μM GST, or 5 μM GST-acocostatin. After 24 h incubation, cells were collected and stained with Annexin V-FITC and PI apoptosis detection kit and analyzed with a flow cytometer. The results are mean ± standard error of the mean of triplicate experiments.

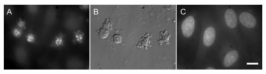

Fig 4.

GST-acocostatin induced chromain fragmentation of HUVEC. (A) Hoechst-stained cells after treatment with 5 μM GST-acocostatin for 12 h. (B) Differential Interference Contrast (DIC) image of cells in (A). (C) Untreated cells stained with Hoechst. Scale bar 10 μM.

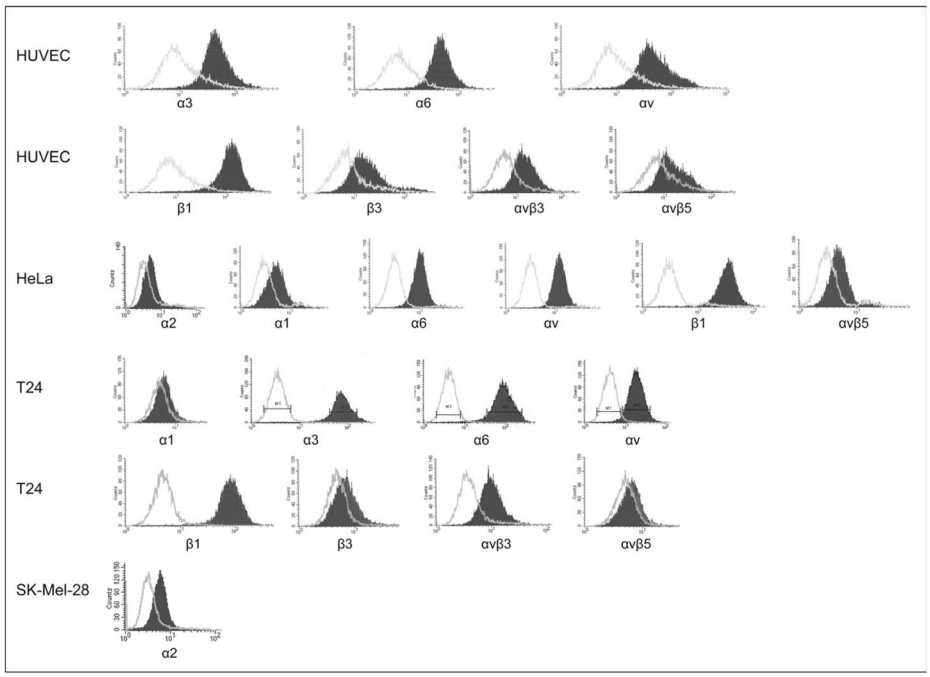

Fig. 5.

Integrin expression of HUVEC, HeLa, and T24 cells. Flow cytometry and human anti-integrin monoclonal antibodies were used to determine integrin expression. Isotype (negative control antibody) profile is indicated as a light gray line. Specific anti-human integrin monoclonal antibody profile is indicated as a gray shaded graph.

Fig. 6.

Amino acid comparison between acocostatin and six PIII disintegrin-like proteins. Dashes indicate amino acid identities as compared to the acocostatin sequence. The disintegrin-like domain is identified with a gray line above its sequence. The variable region is boxed. The first two amino acids of the hypervariable region are identified with asterisks (*). The variable and hypervariable regions are identified according to Takeda et al. (2006) VAP1 crystal structure and alignment analysis.

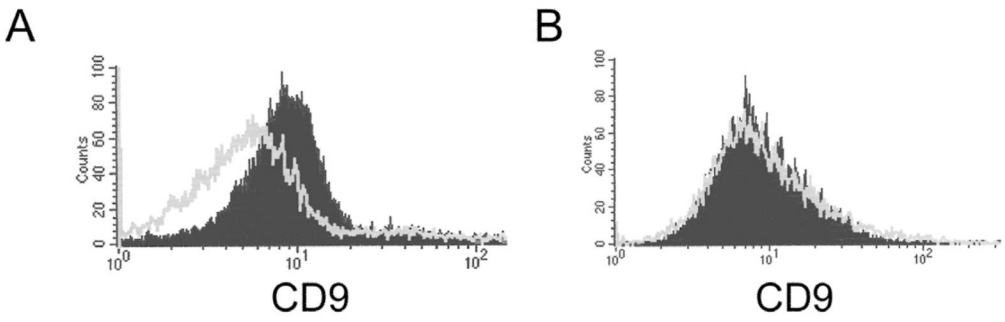

Fig. 7.

CD9 is not expressed on HUVEC. A) Human white blood cells. B) HUVEC. Flow cytometry and human anti-CD9 monoclonal antibodies were used to determine CD9 expression. Isotype (negative control antibody) profile is indicated as a light gray line. Specific anti-human CD9 monoclonal antibody profile is indicated as a gray shaded graph.

Table 1

Inhibition of platelet aggregation with platelet rich plasma (PRP) and whole blood in the presence of GST-acocostatin.

Sample	PRP*	Whole blood*
Control (PBS)	0	0
GST-acocostatin	30	18

The experiments were repeated two times in duplicates. The results are expressed in % of inhibition.

*The final concentration of GST-acocostatin used with PRP and blood was 44 μg/mL

Table 2

Inhibition of SK-MEL-28 and T24 cells migration in presence of GST-acocostatin.

Sample	SK-MEL-28 cells*	T24*
Control (PBS)	0	0
GST-acocostatin	48‡	0

The experiments were repeated three times. The results are expressed in % of inhibition.

*The final concentration of GST-acocostatin used with SK-Mel-28 and T24 cells was 220 μg/mL

‡$p < 0.05$ $p = 0.0036$(Paired t Student).